

Exploring solutions to the muon $g-2$ anomaly in a THDM-like model under flavor constraints

A. Doff^a, João Paulo Pinheiro^b, and C. A. de S. Pires^c

^c*Departamento de Física, Universidade Federal da Paraíba,
Caixa Postal 5008, 58051-970, João Pessoa, PB, Brazil*

^b*Departament de Física Quàntica i Astrofísica and Institut de Ciències del Cosmos,
Universitat de Barcelona, Diagonal 647, E-08028 Barcelona, Spain and*

^a*Universidade Tecnológica Federal do Paraná - UTFPR - DAFIS,
R. Doutor Washington Subtil Chueire,
330 - Jardim Carvalho, 84017-220, Ponta Grossa, PR, Brazil*

(Dated: May 14, 2024)

Abstract

The magnetic moment of the muon can receive significant two-loop contributions from the scalar spectrum in Two Higgs Doublet Models (THDM), particularly for a light pseudoscalar. It is established that the symmetry breaking from $SU(3)_L \times U(1)_N$ to $SU(2)_L \times U(1)_Y$ generates an effective Type-III THDM, which invariably leads to flavor-changing neutral current (FCNC) processes. In this study, we examine whether such an effective THDM framework can account for the anomalous magnetic moment of the muon, considering the constraints imposed by B -meson decays, meson mixing, and invisible Higgs decays. Our principal finding reveals that a pseudoscalar with a mass of 66 GeV and a $\tan \beta$ value of 58 can account for the $g - 2$ anomaly without conflicting with existing experimental limits.

I. INTRODUCTION

The magnetic anomaly of the muon, denoted as $a_\mu = (g - 2)_\mu/2$, has been determined with notable precision by the E821 collaboration at Brookhaven National Laboratory, revealing a discrepancy Δa_μ from the Standard Model prediction by 3.7 standard deviations[1, 2]¹. This discrepancy suggests the necessity for new physics beyond the Standard Model (SM) to explain such deviation. The task of theoretical particle physics is to find scenarios of new physics that provide an explanation to it. Generally, any new physics contributing to a_μ likely involves hypothetical new particles, including vector or scalar bosons, fermions, or pseudoscalars. Some of these particles may contribute positively to a_μ , while others may contribute negatively.

The challenge in resolving the a_μ anomaly arises from the difficulty in balancing the positive and negative contributions to align with the observed value of a_μ . Among the various new contributions, the one from pseudoscalars is singular because, at the one-loop level, it contributes negatively, whereas at the two-loop level, it contributes positively². Thus, explaining a_μ solely with pseudoscalars requires a pseudoscalar with a mass in the tens of GeVs range[4, 5]. Consequently, scenarios featuring pseudoscalars that can accommodate a_μ are highly motivated for further investigation[5–11].

Two Higgs Doublet Models (THDM) [4, 9, 12–16] are very well motivated scenarios for new physics that poses an electroweak scale pseudoscalar in their spectrum of new particles. In THDM, you add another doublet of scalars to the Standard Model and, consequently, the spectrum of scalars get composed by one pair of charged scalar, h_1^\pm , two neutral scalars, h_1 and h_2 , and one pseudoscalar, A [14]. This set of five scalars are intrinsically connected to each other and experimental bounds over one of these particles reflects in bounds to all of them. Each variant of the THDM can reflect different physical consequences, since there are various possibilities of composing Yukawa couplings with two Higgs doublet and the standard fermions multiplets[14, 17]. Usually the new Yukawa couplings are not family universal and can couple differently with each generation. Among the plethora of different THDM, the one that are more constrained by experimental bounds is that where the new doublets interacts exclusively with quarks. The charged scalar can contribute largely to the B -physics observables, imposing indirect constraints in the mass of the new neutral scalars due the potential conditions of the model.

¹A new $g - 2$ experiment with a completely different approach is currently under construction at J-PARC[3]

²The contribution of charged scalars is negative for one-loop and positive for two-loops too, however (in the discussed scenario) as we will present in the text, $m_{h_1^\pm} \geq 483$ GeV, leading to a subdominant contribution (in comparison to A)

In the literature, there are numerous studies on THDM addressing the anomalous magnetic moment of the muon and considering constraints from B -physics[18–23]. However, these studies typically overlook the effects of flavor-changing neutral current (FCNC) interactions. Including FCNC could potentially weaken existing constraints, especially those on the mass of the charged Higgs (h_1^+), which currently stand at over 800 GeV for the Type II THDM variant, for instance. Furthermore, introducing FCNCs can yield significant contributions to flavor-changing neutral processes, such as $M - \bar{M}$ transitions[17]. These constraints can then be used to determine the mixing angles in the Yukawa sector and reduce the number of free parameters, thereby refining constraints on h_1^+ and consequently on A .

On the other hand, it was showed in [24–26] that the variant of THDM called type-III THDM may be realized inside extensions of the standard model based in the $SU(3)_C \times SU(3)_L \times U(1)_N(331)$ symmetry. However, as each version of 331 models possess three variants[27], then each version may generate three what we call 331 inspired THDM.

Regarding 331 models, the extensive investigation done in Ref. [28] showed that no one version of 331 models solve the current muon $g-2$ anomaly³. This finding was based on an energy regime where the 331 models do not revert to Type-III THDM[35] and only single-loop contributions were considered. The motivation for the current study is to explore the muon $g-2$ anomaly within the 331 framework in a regime of energy where Type-III THDM is applicable and taking into account both one- and -two loop contributions under the constraints of flavor physics.

This work is organized in the follow way: in Sec. II we present the 331RHN and its variants. In the Sec. III we calculate the one- and two-loops contributions to Δa_μ . In Sec. IV we obtain the theoretical and experimental constraints on the masses of the scalars that contribute to the $g-2$. In Sec. V we present our numerical analysis and in Sec. VI we present a short discussion followed by the main conclusions.

II. THE 331RHN AND ITS VARIANTS

In order to understand that each version of 331 models dismember in three variants and under which condition each variant generate the effective THDM, we make a short review of the model and how the variants appears. We restrict our study to the 331 model with right-handed

³The simplest extension of the 331RHN that explain Δa_μ at one loop level is by means of the introduction of a sinleg of scalar leptoquark[29]. For other possibilities, see Refs. [28, 30–34]

neutrinos(331RHN)[36, 37].

In the 331RHN the right-handed neutrinos compose the third components of the triplet of leptons,

$$f_{lL} = \begin{pmatrix} \nu_{lL} \\ e_{lL} \\ \nu_{lR}^c \end{pmatrix} \sim (1, 3, -1/3), \quad e_{aR} \sim (1, 1, -1), \quad (1)$$

with $l = e, \mu, \tau$ representing the three SM generations of leptons.

The quark sector also comes in three families. However here there is a peculiarity concerning anomaly cancellation which requires that at least one family of quarks transforms differently from the other two. So we have three variants with each one leading to different physical results. Each variant of the model is presented below.

The gauge sector of the model involves the standard gauge bosons plus one Z' , two new charged gauge bosons W'^{\pm} and two non-hermitian neutral gauge bosons U^0 and $U^{0\prime}$ [38]. All these new gauge bosons must develop mass at TeV scale and due to this their contributions to the a_μ are negligible as showed in Ref.[28].

The scalar sector is composed by the three triplet of scalars $\eta = (\eta^0 \ \eta^- \ \eta'^0)^T$, $\rho = (\rho^+ \ \rho^0 \ \rho'^+)^T$ and $\chi = (\chi^0 \ \chi^- \ \chi'^0)^T$ with η and χ transforming as $(1, 3, -1/3)$ and ρ as $(1, 3, 2/3)$ [39]. After spontaneous breaking of the symmetries, such content of scalar generates masses for all massive particles of the model including fermions and gauge bosons⁴. In order to avoid spontaneous breaking of the lepton number, we assume that only η^0 , ρ^0 , and χ'^0 develop VEV, namely v_η , v_ρ , $v_{\chi'}$ respectively⁵. The potential, the minimum conditions and the spectrum of scalars of the model are found in Ref. (). We just remember here that $v_\eta^2 + v_\rho^2 = v^2$ where v is the standard vev whose value is $(246)^2 \text{GeV}^2$. The vev $v_{\chi'}$ characterizes the energy scale of the breaking of the $SU(3)_L \times U(1)_N$ symmetry. Current LHC bounds imposes $v_{\chi'} \geq 10 \text{TeV}$ [44, 45]. Moreover, we remember that the potential has a trilinear term modulated by the energy parameter f . It is this parameter that decide if the 331 model generates an effective THDM. It was showed in Ref. [35] that this happens only when $f < v_\eta, v_\rho$. For $f \geq v_\eta, v_\rho$ all the spectrum of new scalars, except the Higgs, develop mass at TeV scale. Our interest here is exclusively in the case in which $f < v_\eta, v_\rho, v_{\chi'}$. In it the spectrum of scalars shift in a set of scalar (h_1, h_2, h_1^+, A) with mass at the electroweak scale and a second set of scalars $(H, h_2^+, \eta'^0, \chi'^0)$ with mass at the 331 scale. In the first set of scalars h_1

⁴For the development of the other sectors of the model, see Refs.[27, 40–42]

⁵For the case where the other neutral scalars develop VEVs, see Ref. [43]

play the role of the standard-like Higgs and h_2 is a kind of second Higgs. In it the pseudo scalar A has mass proportional to the trilinear coupling f which means that it may be light as much as f is small. The mass of h_1^+ is determined by the parameter f and couplings of the potential in such a way that it is naturally heavier than A . All this allows we identify this set of scalars as the set of scalars of the 2HDM, but we stress that this is only possible for the case of relative small f . What we do here is to investigate the contributions of this set of scalars to the muon ($g - 2$) at one and two loops in a general way taking into account the contributions of the gauge bosons of the 331RHN inside the variant of the model that enhance the couplings of the charged leptons with the pseudo scalar A by means of $\tan \beta$. In other words, we complement the jobs done in Refs. [24, 28].

Moreover, as feature of 3-3- models we have that anomaly cancellations demand one family of quarks transforming differently from the other two ones. It is this point that generate the variants of the models. In what follow we consider the three variants and separate the main aspect that matter to the calculation of their contributions to the a_μ at one and two loops.

A. Variant I

In this variant the first two families of quarks transform as anti-triplet while the third one transforms as triplet by $SU(3)_L$,

$$\begin{aligned}
Q_{iL} &= \begin{pmatrix} d_i \\ -u_i \\ d'_i \end{pmatrix}_L \sim (3, \bar{3}, 0), u_{iR} \sim (3, 1, 2/3), \\
d_{iR} &\sim (3, 1, -1/3), \quad d'_{iR} \sim (3, 1, -1/3), \\
Q_{3L} &= \begin{pmatrix} u_3 \\ d_3 \\ u'_3 \end{pmatrix}_L \sim (3, 3, 1/3), u_{3R} \sim (3, 1, 2/3), \\
d_{3R} &\sim (3, 1, -1/3), \quad u'_{3R} \sim (3, 1, 2/3),
\end{aligned} \tag{2}$$

where the index $i = 1, 2$ is restricted to only two generations. The negative signal in the anti-triplet Q_{iL} is just to standardise the signals of the charged current interactions with the gauge bosons. The primed quarks are new heavy quarks with the usual $(+\frac{2}{3}, -\frac{1}{3})$ electric charges.

Here the simplest Yukawa interactions that generate the correct mass for all standard quarks are

composed by the terms⁶,

$$-\mathcal{L}_Y \supset g_{ia}^1 \bar{Q}_{iL} \eta^* d_{aR} + h_{3a}^1 \bar{Q}_{3L} \eta u_{aR} + g_{3a}^1 \bar{Q}_{3L} \rho d_{aR} + h_{ia}^1 \bar{Q}_{iL} \rho^* u_{aR} + \text{H.c.}, \quad (3)$$

where $a = 1, 2, 3$ and the parameters g_{ab}^1 and h_{ab}^1 are Yukawa couplings that, for sake of simplification, we consider reals. Observe that in this variant the dominant term that determine the mass of the quark top involves v_η . Than, in this case, it is natural to assume $v_\eta > v_\rho$. With all this in hand, after developing the Yukawa and the scalar sectors as in Refs.[24–26], we obtain the Yukawa interactions terms that give the main contribution at two loops to the $g - 2$ of the muon,

$$\begin{aligned} \mathcal{L}_Y = & i \left(-\frac{\tan \beta}{v} (V_L^u)_{i3} (V_L^u)_{3i} + \frac{\cot \beta}{v} (V_L^u)_{33} (V_L^u)_{33} \right) m_t \bar{t} \gamma_5 t A \\ & + i \left(-\frac{\cot \beta}{v} (V_L^d)_{i3} (V_L^d)_{3i} + \frac{\tan \beta}{v} (V_L^d)_{33} (V_L^d)_{33} \right) m_b \bar{b} \gamma_5 b A \\ & + i \frac{tg\beta}{v} m_l \bar{l} \gamma_5 l A \end{aligned} \quad (4)$$

where the subscripts $i = 1, 2$. The charged leptons are represented by $l = e, \mu, \tau$. The standard vev is $v = 247\text{GeV}$ and $V_L^{u,d}$ are the matrices that mix the left handed quarks. Right-handed quarks are assumed in a diagonal basis. In this variant we define $\tan \beta = \frac{v_\eta}{v_\rho} > 1$.

B. Variant II

In this case the first family transforms as triplet and the second and third family transform as anti-triplet, which means

$$\begin{aligned} Q_{1L} = \begin{pmatrix} u_1 \\ d_1 \\ u'_1 \end{pmatrix}_L & \sim (3, 3, 1/3), u_{1R} \sim (3, 1, 2/3), \\ d_{1R} & \sim (3, 1, -1/3), u'_{iR} \sim (3, 1, 2/3), \\ Q_{iL} = \begin{pmatrix} d_i \\ -u_i \\ d'_i \end{pmatrix}_L & \sim (3, \bar{3}, 0), u_{3R} \sim (3, 1, 2/3), \\ d_{3R} & \sim (3, 1, -1/3), d'_{3R} \sim (3, 1, -1/3), \end{aligned} \quad (5)$$

⁶For the most general Yukawa interactions involving terms that violate lepton number, see: [46].

where the index $i = 2, 3$ is restricted to only two generations.

The minimal set of Yukawa interactions that leads to the correct quark masses involves the terms,

$$\begin{aligned}
- \mathcal{L}_Y \supset & g_{1a}^2 \bar{Q}_{1L} \rho d_{aR} + g_{ia}^2 \bar{Q}_{iL} \eta^* d_{aR} \\
& + h_{1a}^2 \bar{Q}_{1L} \eta u_{aR} + h_{ia}^2 \bar{Q}_{iL} \rho^* u_{aR} + \text{H.c.} .
\end{aligned} \tag{6}$$

Observe that in this case the main contribution to the mass of the quark top is determined by the vev v_ρ . Then in this case we assume $v_\rho > v_\eta$.

Following all the previous procedure done in Variant I, we obtain the following Yukawa interactions among A and the standard quarks and leptons that matter to the calculation of the $g - 2$ of the muon at two loops are given by,

$$\begin{aligned}
\mathcal{L}_Y = & i \left(\frac{\tan \beta}{v} (V_L^u)_{13} (V_L^u)_{33} - \frac{\cot \beta}{v} (V_L^u)_{i3} (V_L^u)_{3i} \right) m_t \bar{t} \gamma_5 t A \\
& + i \left(\frac{\cot \beta}{v} (V_L^d)_{13} (V_L^d)_{31} - \frac{\tan \beta}{v} (V_L^d)_{i3} (V_L^d)_{3i} \right) m_b \bar{b} \gamma_5 b A \\
& + \frac{i}{v \tan \beta} m_l \bar{l} \gamma_5 l A
\end{aligned} \tag{7}$$

where the subscripts $i = 2, 3$. Here we define $\tan \beta = \frac{v_\rho}{v_\eta} > 1$.

C. Variant III

In this case the second family transforms as triplet while the first and third ones transform as anti-triplet

$$\begin{aligned}
Q_{2L} = & \begin{pmatrix} u_2 \\ d_2 \\ u'_2 \end{pmatrix}_L \sim (3, 3, 1/3), u_{2R} \sim (3, 1, 2/3), \\
d_{2R} \sim & (3, 1, -1/3), u'_{2R} \sim (3, 1, 2/3), \\
Q_{iL} = & \begin{pmatrix} d_i \\ -u_i \\ d'_i \end{pmatrix}_L \sim (3, \bar{3}, 0), u_{iR} \sim (3, 1, 2/3), \\
d_{iR} \sim & (3, 1, -1/3), d'_{iR} \sim (3, 1, -1/3),
\end{aligned} \tag{8}$$

where $i = 1, 3$.

Here the Yukawa interactions involve the terms

$$\begin{aligned}
- \mathcal{L}_Y \supset & g_{2a}^3 \bar{Q}_{2L} \rho d_{aR} + g_{ia}^3 \bar{Q}_{iL} \eta^* d_{aR} \\
& + h_{2a}^3 \bar{Q}_{2L} \eta u_{aR} + h_{ia}^3 \bar{Q}_{iL} \rho^* u_{aR} + \text{H.c.},
\end{aligned} \tag{9}$$

where $i = 1, 3$.

Following the procedure of Variant I the interactions of the pseudoscalar A with the standard quarks and leptons that matter to the calculation for the $g - 2$ of the muon at two loops are given by, Coupling: ttA , bbA , llA :

$$\begin{aligned}
\mathcal{L}_Y = & i \left(\frac{\tan \beta}{v} (V_L^u)_{23} (V_L^u)_{32} - \frac{\cot \beta}{v} (V_L^u)_{i3} (V_L^u)_{3i} \right) m_t \bar{t} \gamma_5 t A \\
& + i \left(\frac{\cot \beta}{v} (V_L^d)_{23} (V_L^d)_{32} - \frac{\tan \beta}{v} (V_L^d)_{i3} (V_L^d)_{3i} \right) m_b \bar{b} \gamma_5 b A \\
& + i \frac{m_l}{v \tan \beta} \bar{l} \gamma_5 l A
\end{aligned} \tag{10}$$

where the subscripts $i = 1, 3$, $v = 247\text{GeV}$ and $V^{u,d}$ are the quarks mixing. Here we define $\tan \beta = \frac{v_\rho}{v_\eta} > 1$.

All we showed above tell us that each variant leads to different physical results in what concern flavor physics. Particularly here observe that the differences among the three variants that matter to muon $g - 2$ are the Yukawa interactions of A with the charged leptons l . In the case of variant II and III these interactions are suppressed by $\tan \beta$ while in the variant I it is enhanced by $\tan \beta$. So we deduce that only the variant I has potential to explain Δa_μ at two loops. It is for this reason that from now on we focus exclusively in the variant I of the 331RHN or in its effective THDM formed with this set of Yukawa interactions. Observe that we presented the variants only with the fermions that matter to the calculation of a_μ . In the APPENDIX we present the general Yukawa interactions involving all the set of scalars that compose the THDM for the case of variant I that is the interesting one. To finalize, see that the set of scalars A , h_1 , h_2 , h_1^\pm together with the Yukawa interactions discussed here allow we conclude that the 331RHN in the regime of small f realizes the type-III THDM.

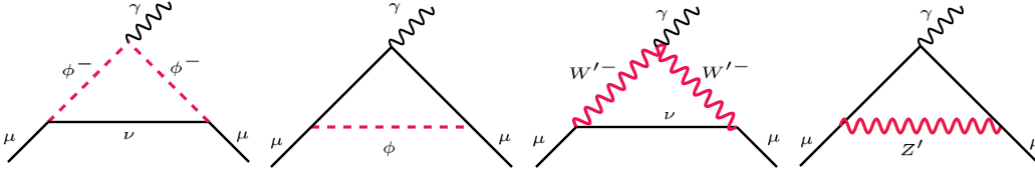


FIG. 1. One-loop contributions to the $g - 2$ of the muon in the 331RHN where ϕ and ϕ^- represent the neutral and charged scalar contributions

III. TWO LOOPS CONTRIBUTIONS TO Δa_μ IN THE EFFECTIVE TYPE-III THDM

Before discuss the two loop case, we first review the main aspects of one loop contributions to a_μ inside the 331RHN. One loop contributions to the muon anomalous magnetic moment in the 331RHN was extensively investigated in [28]. There it was assumed that $\tan \beta = 1$ and that the mixing matrices $V_L^{u,d}$ follow the hierarchy of the CKM one with the main contributions being proportional to $(V_L^{u,d})_{33}$ which was taken to be ≈ 1 . In this case it does not make sense to talk about variants because all the three variants will give the same contributions. The main contributions to Δa_μ at one loop are due to the new gauge bosons W'^{\pm} and Z' , the single charged scalar h_1^+ , the neutral scalar h_2 , and the pseudo scalar A . The set of interactions and their respective contributions to Δa_μ are given in Refs. [28, 47]. The Feynman diagrams due to these contributions are showed in FIG. 1.

As it was extensively discussed in Ref.[28], the 331RHN yields five contributions to $g-2$ with W' giving the dominant positive contribution. The only way the one-loop contribution would accommodate the current prediction of a_μ was if the positive contribution of the W' could surpass the negative ones giving by the scalars and generated the current Δa_μ measurement. This could happen for W' having mass at the electroweak scale which is completely discarded since current LHC bounds demand the gauge bosons of the 331RHN to have mass at the TeV scale. Thus, one loop contributions to the a_μ in the 331RHN is not able to accommodate the current a_μ . In fact in what concern one loop contributions to a_μ in the 331RHN the negative contributions surpass the positive ones. Thus if we want that any new contributions explain Δa_μ we need that the such new contributions surpass the negative net contributions at one loop and provide the current value of Δa_μ

It is very well known that two-loops contributions from pseudo scalars give positive contribution to the a_μ [48],[49], [50] and [51]. The 331RHN has a pseudoscalar, A , in its spectrum

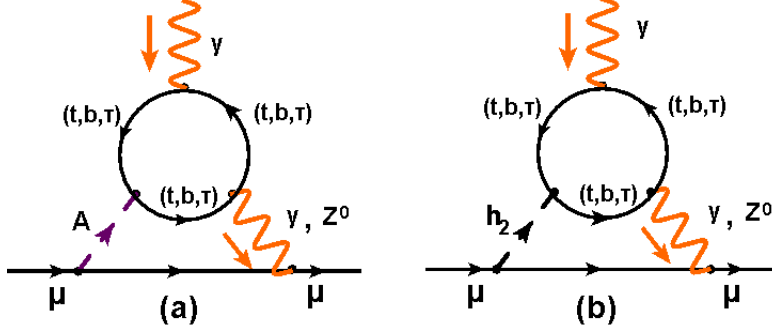


FIG. 2. Two loop Barr-Zee type contributions to the $g - 2$ of the muon in the 331RHN. In this figure h_2 and A represent the neutral scalar and pseudoscalar contributions to $g - 2$ of the muon.

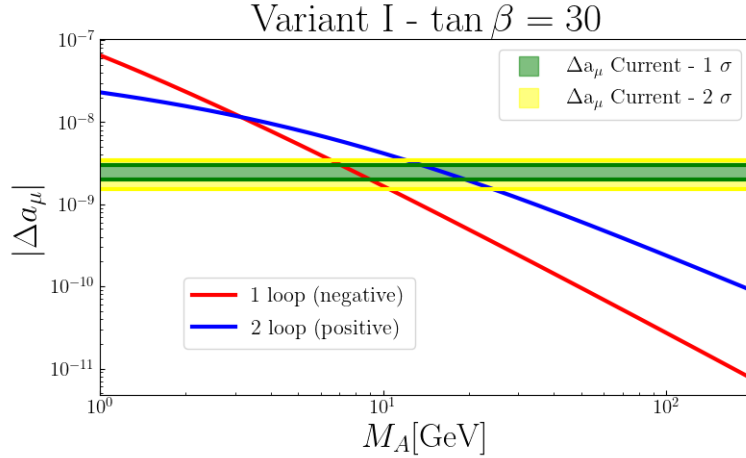


FIG. 3. One and two-loop pseudoscalar contribution for the anomalous $g-2$ of the muon. The green band represents the actual bounds for the anomaly, the red curve represents the module of the one-loop contribution and the blue curve represents the two-loop contribution of the pseudoscalar A .

of scalars. We then ask for what range of values for m_A the contributions of the set of scalars (h_1, h_2, h_1^+, A) at two loops would accommodate the current value of Δa_μ . In the two loops, contributions involving h_1^+, W'^+ and Z' are very suppressed. We neglect them and consider only contributions involving the particles A and h_2 which compose the spectrum of scalar s of type -II THDM. Although the dominant contributions in two loops is due to the pseudoscalar A , we reminder that the contributions due to h_2 , although small, it makes necessary. In other words, they contributions are small but relevant to obtain the desired solution to Δa_μ here.

Following [49], [50], [51] and [48], we will discuss the contributions to a_μ from one and two loops. The expressions for the contributions of one loop is found in Refs. [47] and [28]. For the

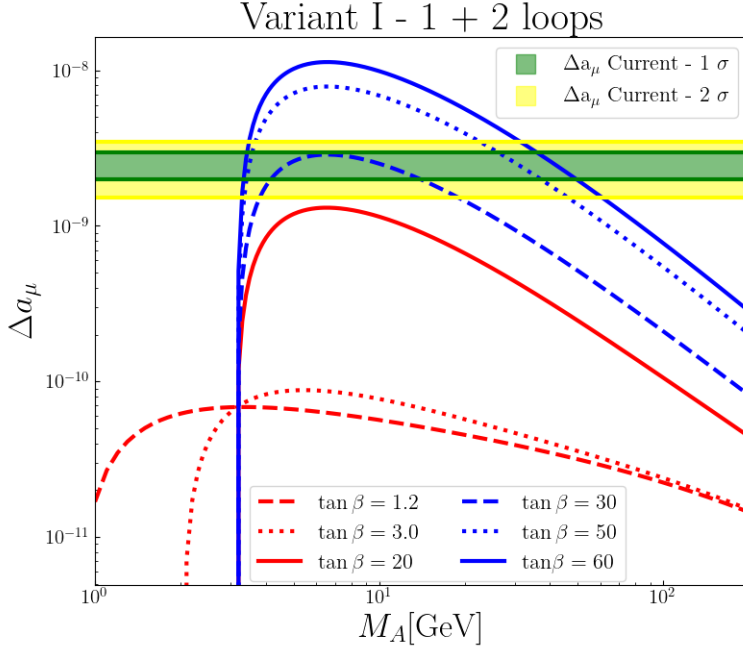


FIG. 4. Here, the curves represent the sum of one and two-loop contributions for the anomalous magnetic moment of the muon for a fixed $\tan \beta$. It is clear that, for $\tan \beta > 27$, it is always possible to find a point in $[M_A, \tan \beta]$ plane that explains the Δa_μ . For more details, see the Appendix.

case of the two loop with A and h_2 we have two dominant contributions, namely one involving γ and other involving Z -boson. The expressions for these contributions are found in Refs. [49], [50] and [51].

In what follows we evaluate such contributions for the variant I of the model as a function of M_A for $\tan \beta = 30$ ⁷. In FIG. (2) we show the Feynman diagrams of the two loop contributions and in FIG. (3) we present our results for the cases of one and two loops. In that figure the red curve represents the module of the one loop contributions while blue curve represents the two loop contributions due to the pseudo scalar A , only, that is definitively positive. The green band represents the current bound for the anomaly. The intersection point of the blue and red curves represents the point where the two loop contributions cancel the net one loop negative contributions. It occurs at $M_A \approx 3$ GeV. From that point ahead the two loops start giving a net positive contribution to Δa_μ . The intersection point of the blue curve with the green band occurs for M_A in the range 15 – 25 GeV. Thus the result presented in FIG. (3) tells us that for A relatively light its two loop contribution surpasses the negative one loop contributions of the spectrum of 331 model that contribute to muon

⁷Here we refer to 331RHN because in one loop we consider the main contribution due to W'^+ .

$g - 2$ and provide the current Δa_μ . The value of M_A in this plot may increase a little as function of $\tan \beta$. We show this in FIG. (4) where we have the behaviour of Δa_μ in function of M_A for various values of $\tan \beta$ considering one and two loops contributions. We have that for $M_A > 3$ GeV and $\tan \beta > 27$ the 331RHN always offers a point in the plane $(M_A, \tan \beta)$ that accommodate the current value of Δa_μ . However to complete our understanding it is recommended to certify what range of values for M_A and $\tan \beta$ accommodate Δa_μ and respect constraints from flavor physics. More precisely we must certify the contributions of A to $K^0 - \bar{K}^0$ and B mesons decay, in addition to the decay $h_1 \rightarrow AA$. We discuss all these constraints right below⁸.

IV. THEORETICAL AND EXPERIMENTAL LIMITS

A. $K^0 - \bar{K}^0$

In the 331RHN the set of neutral particles h_1, h_2, A and Z' contribute to FCNC processes⁹. In the scenario where A solves the muon $g - 2$ anomaly, where it is the lightest of this set of neutral particles, we must worry with its contribution to FCNC processes as meson transitions. Then it makes mandatory to certify if a pseudoscalar with mass of tens of GeVs is in agreement, for example, with the current value of Δm_K associated to the $K^0 - \bar{K}^0$ transition. In this regard, the effective Lagrangian that leads to the $K^0 - \bar{K}^0$ transition can be write as [27]

$$\mathcal{L}_{\text{eff}}^{\mathcal{K}} = -\frac{1}{m_A^2} [\bar{d} (C_K^R P_R - C_K^L P_L) s]^2, \quad (11)$$

where in the equation above $P_{L,R}$ are the left-handed and right-handed projections. In our case the coefficients $C_K^{R,L}$ are obtained from the Yukawa interactions given in Eq.(26) of the APPENDIX. With those interactions we can write

$$\begin{aligned} C_K^R &= (\tan \beta (V_L^d)_{32} (V_L^d)_{13} + \cot \beta (V_L^d)_{i2} (V_L^d)_{1i}) \frac{m_s}{v} \\ C_K^L &= (\tan \beta (V_L^d)_{13}^* (V_L^d)_{32}^* + \cot \beta (V_L^d)_{1i}^* (V_L^d)_{i2}^*) \frac{m_d}{v}. \end{aligned} \quad (12)$$

where $i = 1, 2$.

⁸For previous work addressing a_μ with light pseudo scalar in other variant of the THDM, see Refs. [4, 5]

⁹For important works treating flavor physics in 331 models, see Refs. [52–57]

Assuming the Lagrangian given by Eq.(11) and the coefficients in Eq. (12), and following the procedure described in [27], we obtain the following expression to the mixing parameter Δm_K as function of the coefficients $C_K^{R,L}$

$$\Delta m_K = \frac{2m_K f_k^2}{m_A^2} \left(\frac{5}{24} \text{Re} \left((C_K^L)^2 + (C_K^R)^2 \right) F^2(k) + 2 \text{Re} \left(C_K^L C_K^R \right) G^2(k) \right) \quad (13)$$

where

$$F^2(k) = \left(\frac{m_K}{m_s + m_d} \right)^2$$

$$G^2(k) = \left(\frac{1}{24} + \frac{1}{4} F^2(k) \right).$$

In the Eq.(13) f_K is the kaon(K^0) decay constant and m_k is the kaon mass. The input parameters that will be considered in these equations are listed below

$$m_s = 93.4 \text{ MeV} , m_d = 4.67 \text{ MeV}$$

$$m_K = 497.6 \text{ MeV} , f_K = 156 \text{ MeV}.$$

The coefficients $C_K^{R,L}$ depend on the mixing matrices V_L^d and V_L^u whose entries are unknown free parameters that obey the constraint,

$$V_L^u V_L^{d\dagger} = V_{CKM}, \quad (14)$$

which is not sufficient to fix all the entries of $V_L^{u,d}$. The pattern of $V_L^{u,d}$ involves a high level of arbitrariness. A common procedure in works treating meson transitions is to assume aleatory parametrization to the mixing matrix $V_L^{u,d}$, see for example Refs. [26, 58–60]. However, it was noted in [61] that once the standard-like Higgs contributes inevitably to meson transitions, too, as it is exposed in the Yukawa interactions in Eq. (24), and as its contributions depend exclusively of $V_L^{u,d}$ for fixed angles β and α , it was then realized that the main role of the Higgs contribution to meson transitions is to auxiliar in the choice of the parametrization of the mixing matrices $V_L^{u,d}$.

We then use the following parametrization to the quarks mixing

$$V_L^d = \begin{pmatrix} 0.999986 & 0.005222 & -0.000017 \\ 0.000051 & -0.006463 & 0.999979 \\ 0.005222 & -0.999965 & -0.006464 \end{pmatrix} \quad (15)$$

and

$$V_L^u = \begin{pmatrix} 0.974293 - 0.0000172678 i & 0.00239138 + 0.00330663 i & 0.225311 + 0.0000213748 i \\ -0.224925 - 0.000137852 i & -0.0491546 & 0.973134 \\ 0.0134009 - 0.00322278 i & -0.998789 - 0.0000120136 i & -0.0473675 - 0.000745071 i \end{pmatrix} \quad (16)$$

We checked, following the procedures in Ref. [61], that such pattern of mixing implies that h_1 contribute with 5% to the error of Δm_K^{exp} which is a small fraction of the error. In short, the pattern of mixing above are unitary matrices, generate the current CKM mixing matrix and allow that h_1 get responsible for 5% of the errors of the current measurements of the mass differences Δm_K^{exp} . We then have a realistic parametrization for $V_L^{u,d}$. Throughout this paper we use this parametrization in our calculations.

We are now ready to investigate the effects of a light pseudoscalar, A , in flavor physics. More precisely, we investigate if the $K^0 - \bar{K}^0$ transition is compatible with $M_A \sim (60 - 70)$ GeV's for $\tan \beta \sim 60$ and the pattern of $V_L^{u,d}$ given above. We know that the Standard Model contributions to the neutral meson-anti meson transitions present a good agreement with experiments[62–64]. Furthermore, the uncertainty due to errors in QCD corrections must be considered[65, 66]. Therefore, with regard to the contributions from new physics, it is reasonable to consider that these contributions fall inside the experimental error. In the particular case of the $K^0 - \bar{K}^0$ meson-anti meson transitions we have,

$$\Delta m_K^{exp} = (3.484 \pm 0.006) \times 10^{-12} \text{ MeV}.$$

Based on these considerations, the experimental errors $\delta(\Delta m_K)$ of the $K^0 - \bar{K}^0$ mass difference that we use to constrain new physics is

$$\delta(\Delta m_K) = \pm 0.006 \times 10^{-12} \text{ MeV} = \pm 0.6 \times 10^{-17} \text{ GeV} \quad (17)$$

Once we already considered that h_1 is responsible by 5% of this error, then we assume that the pseudoscalar A will take place of the 95% remaining¹⁰.

We present our results in FIG. (5) where the blue dashed curve corresponds to the behavior of Eq.(13) with M_A under the condition that Δm_K stands for 95% of the error and for the pattern of quark mixing described by Eq.(15) where $i, j = 1, 2, 3$. In that figure the purple band corresponds

¹⁰We stress here that we are aware that the other neutral particles as h_2 and Z' also contribute to such error. However as they are much heavier than A , we think it is reasonable to neglect their contributions to such error[26, 61].

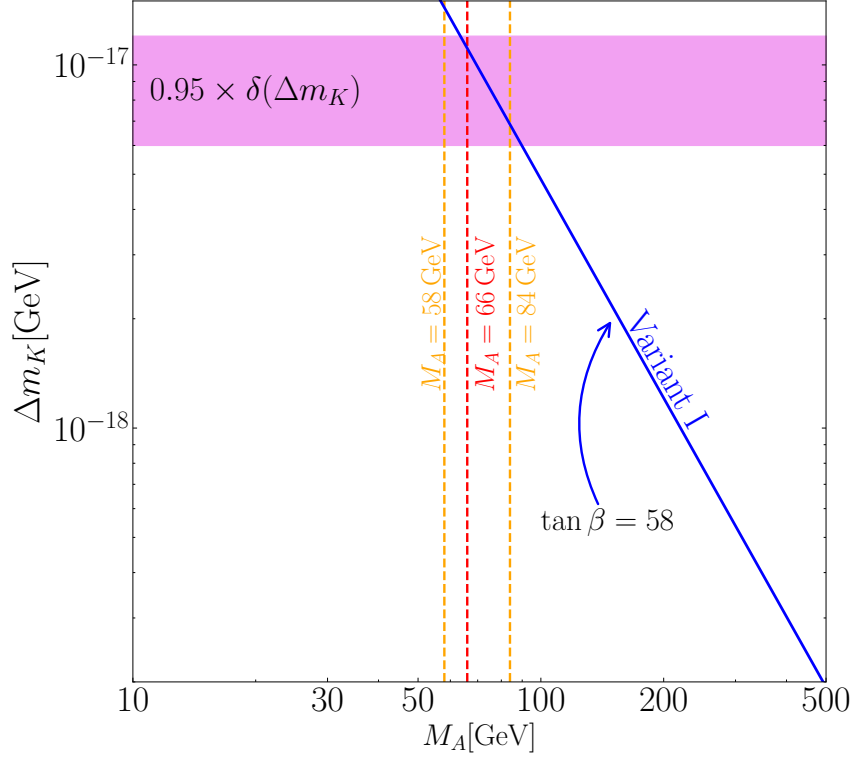


FIG. 5. Flavor changing neutral currents constraint on m_A from $K^0 - \bar{K}^0$ transition. We consider that h_1 is responsible by 5% of $\delta(\Delta m_K)$, and we assume that the pseudoscalar A will take place of the 95% remaining. The contextualization of the curve behavior is described in the text.

to 95% of the error given by Eq.(17) and the dashed red vertical line indicates the position in the band where the pseudoscalar mass, $M_A = 66$ GeV, explains the Δa_μ respecting the constraints by flavor changing neutral processes. In short, we showed that in type-III THDM (or in the 331RHN) there exist a parametrization of the mixing matrices $V_L^{u,d}$ that support a pseudoscalar with mass around 60 GeVs.

B. B-meson decays

Here in this subsection, we will describe important bounds from flavor observables for the THDM type II (and III) [67–74].

1. $B_s \rightarrow \mu\mu$

The $B_s \rightarrow \mu\mu$ decay suffer from few hadronic uncertainties and are induced by FCNC transitions, which make them sensitive probes to the effects of physics beyond the SM, especially models with a non-standard Higgs sector. For our particular case, the process is induced by the gauge bosons Z, W and scalar particles A, h_1, h_2 and h_1^+ . This decay is induced by loop diagrams and any source of FCNC in our theory could in principle contributes to the meson decay. For this analysis, we are using the analytical formulas from [75] and comparing with recent bounds from [76]. One relevant information is that the new vertices that contributes for the diagrams of this decay are proportional to $\cot \beta$, meaning that, for $\tan \beta > 1$, one expect that, for the studied case, the contribution from new physics would be marginal.

2. $B \rightarrow X_s \gamma$

As constantly discussed in the literature, the inclusive radiative decay $B \rightarrow X_s \gamma$ is one of the most important bounds for the mass of a charged scalar in a type II-like THDM[77–81]. The meson decay is generated by the elemental process $b \rightarrow s \gamma$ and since the hadron transition occurs in this process, perturbative QCD corrections are much important and non-perturbative effects must be concerned as well. Here, the Higgs scalar particle gives new contributions to the Wilson coefficients of the effective theory. The process is directly proportional to $\tan \beta$ when h_1^+ is light enough, and this decay figures an important way to bound the mass of the scalar h_1^+ . For sufficiently heavy h_1^+ , the dependence on $\tan \beta$ vanishes. Then, this bound limits inferiorly the mass of h_1^+ .

The bounds are enhanced after calculating the diagrams for more loops. In the literature, there is analytic calculation for NLO in the THDM type II scenario[82]. Recently, a group calculated numerically the NNLO contributions [83] and the constraints on the $m_{h_1^+}$ parameter are extremely strong (> 800 GeV). However, one important assumption of this paper is that they are not considering FCNC at tree-level. As discussed in the literature[14, 71], after including FCNC in the type II THDM, the bounds from the inclusive radiative decay imposed on $m_{h_1^+}$ are relaxed. This is why we are considering in our paper only NLO analytical formulas for the inclusive radiative decay given in [82] and applying the parameterization developed in the $K - \bar{K}^0$ section. The experimental bounds been used are from [76].

3. $B \rightarrow \tau\nu$

Typically in THDM, there are decay processes like $M^\pm \rightarrow \ell\nu_\ell$ mediated by the charged scalar. They occur at tree-level and the most relevant bounds comes from the decays $B \rightarrow \tau\nu$, $D \rightarrow \mu\nu$, $D_s \rightarrow \tau\nu$ and $D \rightarrow \nu\mu$. For the considered case in this article, the strongest contribution is given by the process $B \rightarrow \tau\nu$, and it is very important to obtain a superior limit for $\tan\beta$, at different h_1^+ masses. We performed the analysis applying the experimental limits from [76] at 95% C.L., and the analytical formula from [82].

C. Higgs decay

Concerning The Higgs decay, the coupling

$$\mathcal{L}^{hAA} \supset \frac{1}{2}g_{AAh}h_1AA, \quad \text{where } g_{AAh} = \frac{2v(2\lambda_6(\tan^4\beta + 1) + (\lambda_2 + \lambda_3)\tan^2\beta)}{(\tan^2\beta + 1)^2}, \quad (18)$$

allows the decay mode $h_1 \rightarrow A + A$ when $m_A < m_h/2$. If this is the case, we get

$$\Gamma(h_1 \rightarrow AA) = \frac{g_{hAA}^2}{32\pi m_h} \sqrt{1 - \frac{4m_A^2}{m_{h_1}^2}}.$$

This decay enters in the mode invisible of h_1 . For large values of $\tan\beta$, $g_{hAA} \rightarrow 4\lambda_6v$. Here, λ_6 is a function of the mass of the scalars,

$$\lambda_6 = \frac{m_{h_1}^2}{v^2} - \frac{m_{h_2}^2 - 4M_A^2 \cot\beta}{v^2} \quad (19)$$

and in order to avoid the bounds from the invisible decays of the Higgs, one must artificially reduce the size of λ_6 to be nearly zero or imposes $m_{h_1} = m_{h_2}$, when $\cot\beta \rightarrow 0$. However, without fine tuning, the only way to escape from this bound is to impose an inferior limit for $M_A > \frac{m_h}{2}$. Thus we have to explain Δa_μ with A respecting this bound.

D. Instability conditions

Here we obtain the range of values for the parameters $[M_A, m_{h_1^+}]$ allowed by the stability conditions of the potential[84]. For this we use the most general potential of the 331RHN that conserves lepton number which is given in [85]. In order to avoid spontaneous breaking of the

lepton number, it is assumed that only η^0 , ρ^0 , and χ'^0 develop VEV¹¹. After solving the the mass matrices of the scalars of the model, we obtain the tree-level scalars masses:

$$M_A^2 = \frac{fv_{\chi'}}{4} \left(\frac{\tan \beta}{1 + \tan \beta^2} \frac{v^2}{v_{\chi'}^2} + \tan \beta + \cot \beta \right), m_{h_1^\pm}^2 = \frac{1}{2} \left(fv_{\chi'} + \frac{\lambda_9 \tan \beta}{1 + \tan \beta^2} v^2 \right) (\tan \beta + \cot \beta),$$

$$m_{h_1}^2 = \left(\lambda_2 + \frac{\lambda_6}{2} \right) v^2, \quad m_{h_2}^2 = \left(\lambda_2 - \frac{\lambda_6}{2} \right) v^2 + fv_{\chi'}. \quad (20)$$

These mass expressions and all the other ones are found in [35]. We remember here that f is the energy parameter responsible by the realization of the effective type-III THDM when of the spontaneous breaking of the 331 symmetry.

For the decoupling limit of the heavy 331 particles which means to take $v_{\chi'} \geq 10$ TeV, the phenomenological viable set of scalars are a mixing of ρ and η . After the decoupling, the relevant bounds from below conditions [86] are expressed by the set of relations

$$\lambda_2 > 0, \quad \lambda_3 > 0, \quad \lambda_6 + 2\sqrt{\lambda_2 \lambda_3} > 0, \quad \lambda_6 + \lambda_9 + 2\sqrt{\lambda_2 \lambda_3} > 0, \quad (21)$$

while the unitarity and perturbativity conditions [87] are given by $|\lambda_i| < 4\pi$.

V. NUMERICAL ANALYSIS

In this section, we perform a numerical scan in the parameter space of the effective THDM generated by the Variant I of the 331RHN. Here, we are assuming the limit $v_{\chi} \gg v_{\eta}, v_{\rho}$. This means that, in addition to the SM particles, there are only three new particles, h_2 , h_1^\pm and A . We identify h_1 as the standard Higgs and we are considering the alignment limit for the CP-even scalars [88, 89]. For fixed $v_{\chi} = 10$ TeV and $v = 246$ GeV, and adopting the physical basis for the scalar potential in the 331RHN, there are 4 remaining free parameters that we assume varying in the following range:

$$\{\tan \beta \in [1, 200], m_{h_2} \in [100, 1000] \text{ GeV}, M_A \in [5, 1000] \text{ GeV}, m_{h_1^\pm} \in [100, 1000] \text{ GeV}\}.$$

In FIG. 6, we present the constraints from the processes $B \rightarrow X_s \gamma$ and $B \rightarrow \tau \nu$ in the plane $[m_{h_1^\pm}, \tan \beta]$. It is clear in that figure that $m_{h_1^\pm}$ is bounded from below independently from the value of $\tan \beta$, for $\tan \beta > 1$

$$m_{h_1^\pm} > 483 \text{ GeV},$$

¹¹For the case where the other neutral scalars develop VEVs, see Ref. [46]

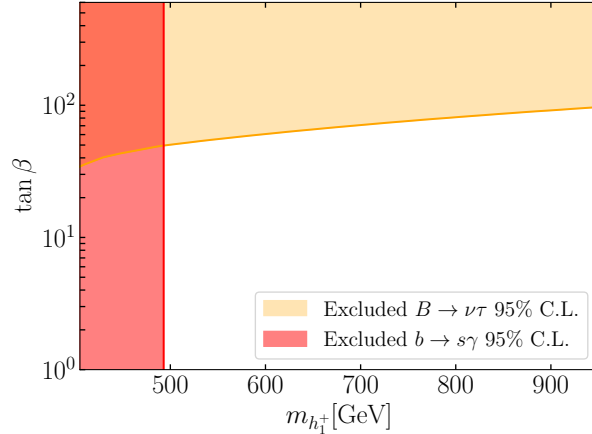


FIG. 6. Excluded regions due to B -meson decays at 95 % C.L. in the $[m_{h_1^+}, \tan \beta]$ plane. From these bounds, we projected these bounds into the $M_A, \tan \beta$ plane without assuming mass degenerescence between h_1^+ and A .

while $B \rightarrow \tau \nu$ limits superiorly the value of $\tan \beta$.

After applying the bounds on the plane $[m_{h_1^+}, \tan \beta]$, one must project these bounds on the $[M_A, \tan \beta]$ plane. But first, we will project the flavor bounds into the $[M_A, m_{h_1^+}]$ plane. This is what is done in FIG. 7. Here, we show the effect of the cumulative bounds from flavor observables in the $[M_A, m_{h_1^+}]$ plane. Here, the blue dots represents the allowed regions after applying the potential bounds (bounded from below conditions (BFB) and unitarity). One interesting fact is that, for high values of $m_{h_1^+}$, M_A is almost degenerated with it. Then, it is impossible to have light A when h_1^+ is a heavy particle due the conditions of the potential. This shows how important are the limits from $B \rightarrow X_s \gamma$. For the same figure, we cumulatively added the bounds from the $B_s \rightarrow \mu \mu$ decay. These bounds are represented by red dots. It was discussed in reference [24] that, for $\tan \beta > 1$, the influence of $B_s \rightarrow \mu \mu$ is marginal. However, one can observe that such statement is not exactly true, there is a non-trivial effect for simultaneous light $m_{h_1^+}$ and M_A . The orange dots represents the previous cumulative bounds together with the allowed region of the inclusive radiative decay $B_s \rightarrow X_s \gamma$. Here it is clear that such bound constrain inferiorly the value of $m_{h_1^+}$, however, it still allows M_A to be small. The green dots represents the previous cumulative bounds together with the allowed region of the tree-level decay $B \rightarrow \tau \nu$. Here, the bound constrains inferiorly the value of M_A and superiorly the value of $\tan \beta$.

In FIG. 8, we projected the discussed bounds from h_1^+ into the $[M_A, \tan \beta]$ plane. Here, we considered the region that explains the anomalous magnetic moment of the muon for one (two) σ

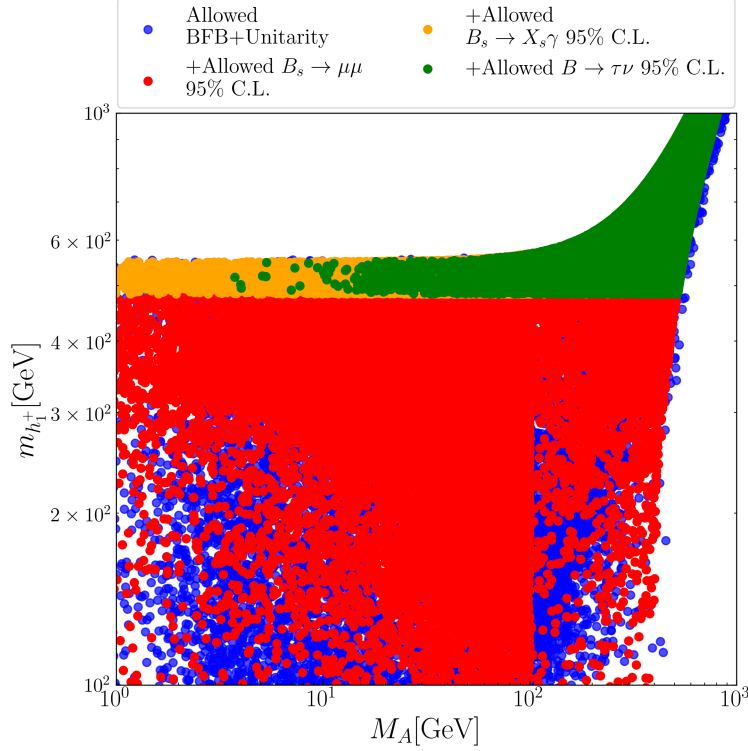


FIG. 7. Here, we can see the relation between the masses of the charged scalar h_1^+ and the pseudoscalar A . The blue dots represents the possible values for masses in the $[M_A, m_{h_1^+}]$ plane in which the potential bounds are obeyed (bounded from below conditions and imposing that the mass of all scalars are positive), red dots represents the cumulative bounds from the muon decays of B_s meson and potential conditions, the yellow dots represents the simultaneous bounds for the decay of B_s into $X_s \gamma$ and previous bounds and the green dots represents the cumulative bounds for the decay of B into $\tau \nu$ and the previous bounds. All flavor observables at 95% C.L..

as the green(yellow) contours. At the same time, as discussed in a previous section, we imposed the bounds from the invisible decay of the Higgs into two A 's. Such bound imposes that $M_A > 62.5$ GeV, independently from the value of $\tan \beta$. After applying all discussed bounds, we discovered a small allowed region that explains the anomalous $g - 2$ and at the same time obeys all main flavor constraints and do not contribute for the Higgs invisible decay.

Then, we can summarize what we did as:

1. For every point in the $[M_A, \tan \beta]$ plane, it is possible to find a parametrization for V_L^d and V_L^u that avoid the constraints from neutral meson-antimeson transitions $K^0 - \bar{K}^0$. Assuming $M_A = 66$ GeV and $\tan \beta = 58$ as a benchmark point, we showed the numerical values of the

unitary matrices V_L^d and V_L^u ;

2. The constraints from $B_s \rightarrow \mu\mu$ are not relevant for the Variant I, when $\tan\beta > 1$, if we simultaneous use bounds from inclusive radiative decay $b \rightarrow s\gamma$;

3. The constraint from $B \rightarrow X_s\gamma$ depend strongly if you consider FCNC. As we discussed, we found the bound:

$$m_{h_1^\pm} > 463 \text{ GeV},$$

fixing the values of V_L^d and V_L^u as described in the text.

4. The tree-level decay of $B \rightarrow \tau\nu$ via charged-scalar exchange limits superiorly the value of $\tan\beta$ and gives an important bound for the plane $[M_A, \tan\beta]$. Increasing the precision of this decay is vital to rule out or not the capability of A to explain the $g - 2$ anomaly and run away from flavour constraints;

5. There is a small window that $(g - 2)_\mu$ can be explained in the effective THDM generated by the Variant I 331RHN. The possible solution for the muon $g - 2$ anomaly that avoids flavor constraints and higgs invisible decay lies on the range $M_A \in [62.5, 122] \text{ GeV}$ for $\tan\beta \in [43, 59]$;

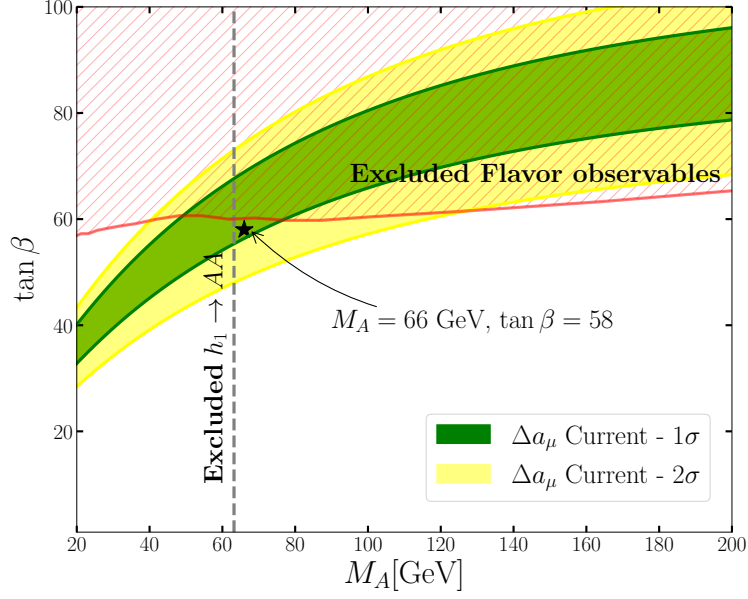


FIG. 8. Imposition of B -physics bounds into the plane $[M_A, \tan \beta]$. The red hatched contour represents the cumulative bounds from the most stringent B -meson decays to limit parameter space of the pseudoscalar A , $B_s \rightarrow X_s \gamma + B_s \rightarrow \mu\mu + B \rightarrow \tau\nu$ at 95% C.L.. The green(yellow) band represents the current bounds from the anomalous magnetic moment of the muon for 1(2) σ . The black star represents one benchmark point that respects the B -physics bounds, the bounds from the invisible decay of the Higgs and explains the Δa_μ in the $[M_A, \tan \beta]$ plane.

VI. DISCUSSION AND CONCLUSION

Explaining the current muon $(g-2)$ anomaly using scalar fields remains a significant challenge. At one-loop levels, charged scalars and pseudoscalars typically contribute negatively, whereas CP-even scalars contribute positively. At two-loop levels, however, all these scalars contribute positively. Individually, each scalar could potentially explain the $(g-2)$ anomaly, but they must be relatively light, which is particularly challenging for charged scalars. Neutral scalars, especially pseudoscalars, are viable candidates as they can be lighter—albeit heavier than $\frac{m_{h_1}}{2}$ to avoid invisible Higgs decays—making them natural candidates to address the $(g-2)$ anomaly.

Pseudoscalars naturally emerge in Two Higgs Doublet Models (THDM) and the 331 model with right-handed neutrinos (331RHN). In regimes where the 331RHN features a light pseudoscalar, it resembles the Type-III THDM. There exists a parameter window where a pseudoscalar mass ranging from 62.5 to 120 GeV, combined with a high $\tan\beta$, successfully explains the muon anomaly. However, this model introduces arbitrariness regarding quark mixing, as the parametrization pattern of $V_L^{u,d}$ cannot be uniquely determined. It is plausible that a suitable parametrization of $V_L^{u,d}$ could allow heavier pseudoscalars as a solution to the $(g-2)$ anomaly, particularly if right-handed quark mixing is considered¹². Thus, the choice of quark mixing pattern significantly influences all flavor physics processes involving scalars, and determining this pattern is crucial for advancing the field and achieving conclusive results in flavor physics.

In conclusion, both the Type-III THDM and the 331 model with right-handed neutrinos explain the muon $(g-2)$ anomaly through dominant two-loop contributions from a pseudoscalar with a mass in the tens of GeV range and a high $\tan\beta$, under the constraints of flavor physics. This positions the 331 model as a compelling framework for exploring new physics beyond the Standard Model.

ACKNOWLEDGMENTS

We thank A. Cherchiglia for valuable discussions. C.A.S.P was supported by the CNPq research grants No. 311936/2021-0. J. P. P. has received support from the European Union’s Horizon 2020 research and innovation program under the Marie Skłodowska-Curie grant agreement No 860881-HIDDeN.

¹²Paper in progress.

VII. APPENDIX

A. One-loop contribution

For the case of the variant I, we have the following Yukawa interactions among h_1^+ and the quarks

$$\begin{aligned} \mathcal{L} \supset & \sqrt{2}h_1^+ \left(-\frac{\cot\beta}{v}(V_L^d)_{ia}(V_L^u)_{bi} + \frac{\tan\beta}{v}(V_L^d)_{3a}(V_L^u)_{b3} \right) (m_{down})_a \bar{\hat{u}}_{bL} \hat{d}_{aR} \\ & + \sqrt{2}h_1^- \left(-\frac{\tan\beta}{v}(V_L^u)_{ia}(V_L^d)_{bi} + \frac{\cot\beta}{v}(V_L^u)_{3a}(V_L^d)_{b3} \right) (m_{up})_a \bar{\hat{d}}_{bL} \hat{u}_{aR} + H.c. \end{aligned} \quad (22)$$

where the subscripts $i = 1, 2$ and $a, b = 1, 2, 3$ with $(m_{down})_{1,2,3} = (m_d, m_s, m_b)$ and $(m_{up})_{1,2,3} = (m_u, m_c, m_t)$. The fields $\hat{u}_{L,R} = (u_{L,R}, c_{L,R}, t_{L,R})$ and $\hat{d}_{L,R} = (d_{L,R}, s_{L,R}, b_{L,R})$. Assuming the expression above and Eqs.(15) and (16), the effective Yukawa $y_{h_1^+}^t$ coupling of the quark top with h_1^+ can be written as

$$y_{h_1^+}^t = 0.973 \tan\beta \frac{m_t}{v} - 0.0002 \cot\beta \frac{m_t}{v} \approx 0.973 \tan\beta \frac{m_t}{v}. \quad (23)$$

Yukawa interactions with the higgses h_1 and h_2

$$\begin{aligned} \mathcal{L} \supset & \frac{\sqrt{1 + \tan^2\beta^2}}{\tan\beta v} [c_\alpha (V_L^d)_{ia}(V_L^d)_{bi} + s_\alpha \tan\beta (V_L^d)_{3a}(V_L^d)_{b3}] (m_{down})_a \bar{\hat{d}}_{bL} \hat{d}_{aR} h_1 \\ & + \frac{\sqrt{1 + \tan^2\beta^2}}{\tan\beta v} [s_\alpha \tan\beta (V_L^u)_{ia}(V_L^u)_{bi} + c_\alpha (V_L^u)_{3a}(V_L^u)_{b3}] (m_{up})_a \bar{\hat{u}}_{bL} \hat{u}_{aR} h_1 + H.c, \end{aligned} \quad (24)$$

and

$$\begin{aligned} \mathcal{L} \supset & \frac{\sqrt{1 + \tan^2\beta^2}}{\tan\beta v} [-s_\alpha (V_L^d)_{ia}(V_L^d)_{bi} + c_\alpha \tan\beta (V_L^d)_{3a}(V_L^d)_{b3}] (m_{down})_a \bar{\hat{d}}_{bL} \hat{d}_{aR} h_2 \\ & + \frac{\sqrt{1 + \tan^2\beta^2}}{\tan\beta v} [-c_\alpha \tan\beta (V_L^u)_{ia}(V_L^u)_{bi} - s_\alpha (V_L^u)_{3a}(V_L^u)_{b3}] (m_{up})_a \bar{\hat{u}}_{bL} \hat{u}_{aR} h_2 + H.c. \end{aligned} \quad (25)$$

where $s_\alpha = \sin\alpha$ and $c_\alpha = \cos\alpha$ are the mixing angle among the neutral higgses.

The Yukawa interactions with A is given by

$$\begin{aligned} \mathcal{L}_Y^A = & iA\bar{\hat{u}}_{bL} \left(-\frac{\tan\beta}{v}(V_L^u)_{ia}(V_L^u)_{bi}(m_{up})_a + \frac{\cot\beta}{v}(V_L^u)_{3a}(V_L^u)_{b3}(m_{up})_a \right) \hat{u}_{aR} \\ & + iA\bar{\hat{d}}_{bL} \left(\frac{\cot\beta}{v}(V_L^d)_{ia}(V_L^d)_{bi}(m_{down})_a + \frac{\tan\beta}{v}(V_L^d)_{3a}(V_L^d)_{b3}(m_{down})_a \right) \hat{d}_{aR} + H.c. \end{aligned} \quad (26)$$

the indexes $i = 1, 2$ and $a, b = 1, 2, 3$ were defined in the previous expressions. Considering the expression above and Eqs.(15) and (16), the effective Yukawa y_A^t coupling of the quark top with A can be written as

$$y_A^t = 0.973 \tan\beta \frac{m_t}{v} + 0.0012 \cot\beta \frac{m_t}{v} \approx 0.973 \tan\beta \frac{m_t}{v}. \quad (27)$$

B. One and two-loop contribution of CP-odd scalar

The light CP-odd scalars negative one-loop contribution for the anomalous magnetic moment of the muon is given by:

$$\Delta a_\mu(A)^{(1\text{-loop})} = -\frac{m_\mu^2}{8\pi^2 M_A^2} \left(\frac{g^2 m_\mu^2 A_\mu^2}{4M_W^2} \right) H\left(\frac{m_\mu^2}{M_A^2}\right), \quad (28)$$

such that $H(y) = \int_0^1 \frac{x^3 dx}{1-x+x^2 y}$. The light CP-odd scalars positive two-loop contribution for the anomalous magnetic moment of the muon is given by:

$$\Delta a_\mu(A)^{(2\text{-loop})} = \Delta a_\mu(A)_\gamma^{(2\text{-loop})} + \Delta a_\mu(A)_Z^{(2\text{-loop})}, \quad (29)$$

such that:

$$\Delta a_\mu(A)_\gamma^{(2\text{-loop})} = \frac{\alpha^2}{8\pi^2 \sin^2 \theta_W} \frac{m_\mu^2 A_\mu}{M_W^2} \sum_{f=t,b,\tau} N_c^f q_f^2 A_f \frac{m_f^2}{M_A^2} \mathcal{F}\left(\frac{m_f^2}{M_A^2}\right) \quad (30)$$

and

$$\Delta a_\mu(A)_Z^{(2\text{-loop})} = \frac{\alpha^2 m_\mu^2 A_\mu g_V^\mu}{8\pi^2 \sin^4 \theta_W \cos^4 \theta_W M_Z^2} \sum_{f=t,b,\tau} \frac{N_c^f g_V^f q_f A_f m_f^2}{M_Z^2 - M_A^2} \left[\mathcal{F}\left(\frac{m_f^2}{M_Z^2}\right) - \mathcal{F}\left(\frac{m_f^2}{M_A^2}\right) \right] \quad (31)$$

such that $g_V^f = \frac{1}{2}T_3(f_L) - q_f \sin^2 \theta_W$ and $\mathcal{F}(x) = \int_0^1 dz \ln\left(\frac{x}{z(1-z)}\right) \frac{1}{x-z(1-z)}$.

We performed the full calculation using the analytical formulas from [50], adding charged and CP-even scalars too.

C. Asymptotic Limits

Analyzing FIG. 4, it is possible to observe, for sufficiently high values of $\tan \beta$, a particular value of M_A in which the 2-loop contribution for the $g - 2$ of the muon becomes dominant in relation to the 1-loop one.

Here in this appendix, we will try to estimate analytically which value of M_A the two-loop contribution becomes dominant. One first observation is that $\Delta a_\mu(A)_Z^{(2\text{-loop})}$ is always suppressed in relation to $\Delta a_\mu(A)_\gamma^{(2\text{-loop})}$. Then, it is sufficient to understand the limit in which the photon Barr-Zee contribution is larger than the negative one-loop contribution, or, $\Delta a_\mu(A)_\gamma^{(2\text{-loop})} + \Delta a_\mu(A)^{(1\text{-loop})} = 0$.

Using equations 28 and 30, we will obtain the approximated equation:

$$\frac{1}{3}m_b^2\mathcal{F}\left(\frac{m_b^2}{M_A}\right) + \frac{4}{3\tan^4\beta}m_t^2\ln\left(\frac{m_t^2}{M_A^2}\right) + m_\tau^2\mathcal{F}\left(\frac{m_\tau^2}{M_A}\right) = \frac{g^2s_W^2m_\mu^2}{4\alpha^2}H\left(\frac{m_\mu^2}{M_A^2}\right) \quad (32)$$

For $\tan\beta$ larger than one and smaller than 5, the top-quark contribution is relevant to the total magnetic moment of the muon. However, for such small values of $\tan\beta$, it is not possible for A to explain the anomaly(FIG. 4). For $\tan\beta > 5$, the top-quark contribution is irrelevant to the total magnetic moment of the muon. Not only that, $\Delta a_\mu(A)^{(2\text{-loop})} = -\Delta a_\mu(A)^{(1\text{-loop})}$ becomes independent of $\tan\beta$, as observed in FIG. 4, too.

Now, solving numerically:

$$\frac{1}{3}m_b^2\mathcal{F}\left(\frac{m_b^2}{M_A}\right) + m_\tau^2\mathcal{F}\left(\frac{m_\tau^2}{M_A}\right) = \frac{g^2s_W^2m_\mu^2}{4\alpha^2}H\left(\frac{m_\mu^2}{M_A^2}\right) \quad (33)$$

leads to $M_A \approx 3.16$ GeV, explaining the shape of the figures in FIG. 4.

-
- [1] D. P. Aguillard et al. Measurement of the Positive Muon Anomalous Magnetic Moment to 0.20 ppm. *Phys. Rev. Lett.*, 131(16):161802, 2023. doi:10.1103/PhysRevLett.131.161802.
 - [2] B. Abi et al. Measurement of the Positive Muon Anomalous Magnetic Moment to 0.46 ppm. *Phys. Rev. Lett.*, 126(14):141801, 2021. doi:10.1103/PhysRevLett.126.141801.
 - [3] M. Abe et al. A New Approach for Measuring the Muon Anomalous Magnetic Moment and Electric Dipole Moment. *PTEP*, 2019(5):053C02, 2019. doi:10.1093/ptep/ptz030.
 - [4] Alessandro Broggio, Eung Jin Chun, Massimo Passera, Ketan M. Patel, and Sudhir K. Vempati. Limiting two-Higgs-doublet models. *JHEP*, 11:058, 2014. doi:10.1007/JHEP11(2014)058.
 - [5] Tao Han, Sin Kyu Kang, and Joshua Sayre. Muon $g - 2$ in the aligned two Higgs doublet model. *JHEP*, 02:097, 2016. doi:10.1007/JHEP02(2016)097.
 - [6] Lei Wang and Xiao-Fang Han. A light pseudoscalar of 2HDM confronted with muon $g-2$ and experimental constraints. *JHEP*, 05:039, 2015. doi:10.1007/JHEP05(2015)039.
 - [7] Tomohiro Abe, Ryosuke Sato, and Kei Yagyu. Lepton-specific two Higgs doublet model as a solution of muon $g - 2$ anomaly. *JHEP*, 07:064, 2015. doi:10.1007/JHEP07(2015)064.
 - [8] Andreas Crivellin, Julian Heeck, and Peter Stoffer. A perturbed lepton-specific two-Higgs-doublet

- model facing experimental hints for physics beyond the Standard Model. *Phys. Rev. Lett.*, 116(8): 081801, 2016. doi:10.1103/PhysRevLett.116.081801.
- [9] Eung Jin Chun and Jinsu Kim. Leptonic Precision Test of Leptophilic Two-Higgs-Doublet Model. *JHEP*, 07:110, 2016. doi:10.1007/JHEP07(2016)110.
- [10] Victor Ilisie. New Barr-Zee contributions to $(g - 2)_\mu$ in two-Higgs-doublet models. *JHEP*, 04:077, 2015. doi:10.1007/JHEP04(2015)077.
- [11] Adriano Cherchiglia, Dominik Stöckinger, and Hyejung Stöckinger-Kim. The muon $g-2$ for low-mass pseudoscalar Higgs in the general 2HDM. *EPJ Web Conf.*, 179:01022, 2018. doi: 10.1051/epjconf/201817901022.
- [12] Gautam Bhattacharyya and Dipankar Das. Scalar sector of two-Higgs-doublet models: A minireview. *Pramana*, 87(3):40, 2016. doi:10.1007/s12043-016-1252-4.
- [13] Lei Wang, Feng Zhang, and Xiao-Fang Han. Two-higgs-doublet model of type ii confronted with the lhc run i and run ii data. *Physical Review D*, 95(11):115014, 2017. doi:10.1103/PhysRevD.95.115014.
- [14] G. C. Branco, P. M. Ferreira, L. Lavoura, M. N. Rebelo, Marc Sher, and Joao P. Silva. Theory and phenomenology of two-Higgs-doublet models. *Phys. Rept.*, 516:1–102, 2012. doi: 10.1016/j.physrep.2012.02.002.
- [15] A. Barroso, P. M. Ferreira, and R. Santos. Electroweak symmetry breaking and scalar singlets in two-higgs-doublet models. *Physical Review D*, 74(8):085016, 2006.
- [16] Debtosh Chowdhury and Otto Eberhardt. Global fits of the two-loop renormalized Two-Higgs-Doublet model with soft Z_2 breaking. *JHEP*, 11:052, 2015. doi:10.1007/JHEP11(2015)052.
- [17] Andreas Crivellin, Ahmet Kokulu, and Christoph Greub. Flavor-phenomenology of two-Higgs-doublet models with generic Yukawa structure. *Phys. Rev. D*, 87(9):094031, 2013. doi: 10.1103/PhysRevD.87.094031.
- [18] Peter Athron, Csaba Balázs, Douglas H. J. Jacob, Wojciech Kotlarski, Dominik Stöckinger, and Hyejung Stöckinger-Kim. New physics explanations of a_μ in light of the FNAL muon $g - 2$ measurement. *JHEP*, 09:080, 2021. doi:10.1007/JHEP09(2021)080.
- [19] G. G. Boyarkina and O. M. Boyarkin. The $(g - 2)_\mu$ anomaly, Higgs bosons and heavy neutrinos. *Phys. Rev. D*, 67:073023, 2003. doi:10.1103/PhysRevD.67.073023.
- [20] Chuan-Hung Chen, Cheng-Wei Chiang, and Takaaki Nomura. Muon $g-2$ in a two-Higgs-doublet model with a type-II seesaw mechanism. *Phys. Rev. D*, 104(5):055011, 2021. doi: 10.1103/PhysRevD.104.055011.

- [21] F. Larios, G. Tavares-Velasco, and C. P. Yuan. A Very light CP odd scalar in the two Higgs doublet model. *Phys. Rev. D*, 64:055004, 2001. doi:10.1103/PhysRevD.64.055004.
- [22] Shao-Ping Li, Xin-Qiang Li, Yuan-Yuan Li, Ya-Dong Yang, and Xin Zhang. Power-aligned 2HDM: a correlative perspective on $(g - 2)_{e,\mu}$. *JHEP*, 01:034, 2021. doi:10.1007/JHEP01(2021)034.
- [23] Nabarun Chakrabarty, Ujjal Kumar Dey, and Biswarup Mukhopadhyaya. High-scale validity of a two-Higgs doublet scenario: a study including LHC data. *JHEP*, 12:166, 2014. doi:10.1007/JHEP12(2014)166.
- [24] A. L. Cherchiglia and O. L. G. Peres. On the viability of a light scalar spectrum for 3-3-1 models. *JHEP*, 04:017, 2023. doi:10.1007/JHEP04(2023)017.
- [25] Zhiyi Fan and Kei Yagyu. CP-violating 2HDMs emerging from 3-3-1 models. *JHEP*, 06:014, 2022. doi:10.1007/JHEP06(2022)014.
- [26] Hiroshi Okada, Nobuchika Okada, Yuta Orikasa, and Kei Yagyu. Higgs phenomenology in the minimal $SU(3)_L \times U(1)_X$ model. *Phys. Rev. D*, 94(1):015002, 2016. doi:10.1103/PhysRevD.94.015002.
- [27] Vinícius Oliveira and C. A. de S. Pires. Flavor changing neutral current processes and family discrimination in 3-3-1 models. *J. Phys. G*, 50(11):115002, 2023. doi:10.1088/1361-6471/acf1b7.
- [28] Álvaro S. de Jesus, Sergey Kovalenko, Farinaldo S. Queiroz, Carlos A. de S. Pires, and Yoxara S. Villamizar. Dead or alive? Implications of the muon anomalous magnetic moment for 3-3-1 models. *Phys. Lett. B*, 809:135689, 2020. doi:10.1016/j.physletb.2020.135689.
- [29] A. Doff and C. A. de S. Pires. Introducing scalar leptoquarks into a 3-3-1 model to solve the $(g - 2)_\mu$ puzzle. 3 2024.
- [30] T. T. Hong, L. T. T. Phuong, T. Phong Nguyen, N. H. T. Nha, and L. T. Hue. $(g - 2)_{e,\mu}$ anomalies and decays $h, Z \rightarrow e_b e_a$ in 3-3-1 models with inverse seesaw neutrinos. 4 2024.
- [31] João Paulo Pinheiro, C. A. de S. Pires, Farinaldo S. Queiroz, and Yoxara S. Villamizar. Confronting the inverse seesaw mechanism with the recent muon $g-2$ result. *Phys. Lett. B*, 823:136764, 2021. doi:10.1016/j.physletb.2021.136764.
- [32] Chris Kelso, H. N. Long, R. Martinez, and Farinaldo S. Queiroz. Connection of $g - 2_\mu$, electroweak, dark matter, and collider constraints on 331 models. *Phys. Rev. D*, 90(11):113011, 2014. doi:10.1103/PhysRevD.90.113011.
- [33] Nguyen Anh Ky, Hoang Ngoc Long, and Dang Van Soa. Anomalous magnetic moment of muon in 3 3 1 models. *Phys. Lett. B*, 486:140–146, 2000. doi:10.1016/S0370-2693(00)00696-1.
- [34] A. E. Cárcamo Hernández, Yocelyne Hidalgo Velásquez, Sergey Kovalenko, H. N. Long, Nicolás A.

- Pérez-Julve, and V. V. Vien. Fermion spectrum and $g - 2$ anomalies in a low scale 3-3-1 model. *Eur. Phys. J. C*, 81(2):191, 2021. doi:10.1140/epjc/s10052-021-08974-4.
- [35] Joao Paulo Pinheiro and C. A. de S. Pires. On the Higgs spectra of the 3-3-1 model. *Phys. Lett. B*, 836:137584, 2023. doi:10.1016/j.physletb.2022.137584.
- [36] Robert Foot, Hoang Ngoc Long, and Tuan A. Tran. $SU(3)_L \otimes U(1)_N$ and $SU(4)_L \otimes U(1)_N$ gauge models with right-handed neutrinos. *Phys. Rev. D*, 50(1):R34–R38, 1994. doi:10.1103/PhysRevD.50.R34.
- [37] J. C. Montero, F. Pisano, and V. Pleitez. Neutral currents and GIM mechanism in $SU(3)_L \times U(1)_N$ models for electroweak interactions. *Phys. Rev. D*, 47:2918–2929, 1993. doi:10.1103/PhysRevD.47.2918.
- [38] Hoang Ngoc Long. $SU(3)_L \times U(1)_N$ model for right-handed neutrino neutral currents. *Phys. Rev. D*, 54:4691–4693, 1996. doi:10.1103/PhysRevD.54.4691.
- [39] Hoang Ngoc Long. Scalar sector of the 3 3 1 model with three Higgs triplets. *Mod. Phys. Lett. A*, 13:1865–1874, 1998. doi:10.1142/S0217732398001959.
- [40] Hoang Ngoc Long. The 331 model with right handed neutrinos. *Phys. Rev. D*, 53:437–445, 1996. doi:10.1103/PhysRevD.53.437.
- [41] Hoang Ngoc Long and D. V. Soa. Gauge boson self-interactions in the $SU(3)_C \times SU(3)_L \times U(1)_N$ models. In *32nd Rencontres de Moriond: Electroweak Interactions and Unified Theories*, pages 249–255, 1997.
- [42] Qing-Hong Cao and Dong-Ming Zhang. Collider Phenomenology of the 3-3-1 Model. 11 2016.
- [43] C. A. de S. Pires and P. S. Rodrigues da Silva. Spontaneous breaking of global symmetries and invisible triplet Majoron. *Eur. Phys. J. C*, 36:397–403, 2004. doi:10.1140/epjc/s2004-01949-3.
- [44] Y. A. Coutinho, V. Salustino Guimarães, and A. A. Nepomuceno. Bounds on Z' from 3-3-1 model at the LHC energies. *Phys. Rev. D*, 87(11):115014, 2013. doi:10.1103/PhysRevD.87.115014.
- [45] A. Alves, L. Duarte, S. Kovalenko, Y. M. Oviedo-Torres, F. S. Queiroz, and Y. S. Villamizar. Constraining 3-3-1 models at the LHC and future hadron colliders. *Phys. Rev. D*, 106(5):055027, 2022. doi:10.1103/PhysRevD.106.055027.
- [46] A. Doff, C. A. de S. Pires, and P. S. Rodrigues da Silva. Spontaneous CP violation in the 3-3-1 model with right-handed neutrinos. *Phys. Rev. D*, 74:015014, 2006. doi:10.1103/PhysRevD.74.015014.
- [47] Manfred Lindner, Moritz Platscher, and Farinaldo S. Queiroz. A Call for New Physics : The Muon Anomalous Magnetic Moment and Lepton Flavor Violation. *Phys. Rept.*, 731:1–82, 2018. doi:

- 10.1016/j.physrep.2017.12.001.
- [48] Adriano Cherchiglia, Patrick Kneschke, Dominik Stöckinger, and Hyejung Stöckinger-Kim. The muon magnetic moment in the 2HDM: complete two-loop result. *JHEP*, 01:007, 2017. doi:10.1007/JHEP10(2021)242. [Erratum: JHEP 10, 242 (2021)].
- [49] Darwin Chang, We-Fu Chang, Chung-Hsien Chou, and Wai-Yee Keung. Large two loop contributions to $g-2$ from a generic pseudoscalar boson. *Phys. Rev. D*, 63:091301, 2001. doi:10.1103/PhysRevD.63.091301.
- [50] Eung Jin Chun, Jongkuk Kim, and Tanmoy Mondal. Electron EDM and Muon anomalous magnetic moment in Two-Higgs-Doublet Models. *JHEP*, 12:068, 2019. doi:10.1007/JHEP12(2019)068.
- [51] P. M. Ferreira, B. L. Gonçalves, F. R. Joaquim, and Marc Sher. $(g-2)_\mu$ in the 2HDM and slightly beyond: An updated view. *Phys. Rev. D*, 104(5):053008, 2021. doi:10.1103/PhysRevD.104.053008.
- [52] Christoph Promberger, Sebastian Schatt, and Felix Schwab. Flavor Changing Neutral Current Effects and CP Violation in the Minimal 3-3-1 Model. *Phys. Rev. D*, 75:115007, 2007. doi:10.1103/PhysRevD.75.115007.
- [53] Richard H. Benavides, Yithsbey Giraldo, and William A. Ponce. FCNC in the 3-3-1 model with right-handed neutrinos. *Phys. Rev. D*, 80:113009, 2009. doi:10.1103/PhysRevD.80.113009.
- [54] Andrzej J. Buras, Fulvia De Fazio, Jennifer Girrbach, and Maria V. Carlucci. The Anatomy of Quark Flavour Observables in 331 Models in the Flavour Precision Era. *JHEP*, 02:023, 2013. doi:10.1007/JHEP02(2013)023.
- [55] Andrzej J. Buras, Fulvia De Fazio, and Jennifer Girrbach. 331 models facing new $b \rightarrow s\mu^+\mu^-$ data. *JHEP*, 02:112, 2014. doi:10.1007/JHEP02(2014)112.
- [56] Andrzej J. Buras and Fulvia De Fazio. 331 model predictions for rare B and K decays, and $\Delta F = 2$ processes: an update. *JHEP*, 03:219, 2023. doi:10.1007/JHEP03(2023)219.
- [57] Duy Nguyen Tuan, Takeo Inami, and Huong Do Thi. Physical constraints derived from FCNC in the 3-3-1-1 model. *Eur. Phys. J. C*, 81(9):813, 2021. doi:10.1140/epjc/s10052-021-09583-x.
- [58] D. Cogollo, A. Vital de Andrade, F. S. Queiroz, and P. Rebello Teles. Novel sources of Flavor Changed Neutral Currents in the 331_{RHN} model. *Eur. Phys. J. C*, 72:2029, 2012. doi:10.1140/epjc/s10052-012-2029-7.
- [59] Farinaldo S. Queiroz, Clarissa Siqueira, and José W. F. Valle. Constraining Flavor Changing Interactions from LHC Run-2 Dilepton Bounds with Vector Mediators. *Phys. Lett. B*, 763:269–274, 2016. doi:10.1016/j.physletb.2016.10.057.

- [60] A. E. Cárcamo Hernández, L. Duarte, A. S. de Jesus, S. Kovalenko, F. S. Queiroz, C. Siqueira, Y. M. Oviedo-Torres, and Y. Villamizar. Flavor changing interactions confronted with meson mixing and hadron colliders. *Phys. Rev. D*, 107(6):063005, 2023. doi:10.1103/PhysRevD.107.063005.
- [61] Vinícius Oliveira and C. A. de S. Pires. Bounds on quark mixing, MZ' and $Z - Z'$ mixing angle from flavor changing neutral processes in a 3-3-1 model. *Phys. Lett. B*, 846:138216, 2023. doi:10.1016/j.physletb.2023.138216.
- [62] Gerhard Buchalla, Andrzej J. Buras, and Markus E. Lautenbacher. Weak decays beyond leading logarithms. *Rev. Mod. Phys.*, 68:1125–1144, 1996. doi:10.1103/RevModPhys.68.1125.
- [63] Luca Di Luzio, Matthew Kirk, Alexander Lenz, and Thomas Rauh. ΔM_s theory precision confronts flavour anomalies. *JHEP*, 12:009, 2019. doi:10.1007/JHEP12(2019)009.
- [64] Kristof De Bruyn, Robert Fleischer, Eleftheria Malami, and Philine van Vliet. New physics in B_q^{0-} mixing: present challenges, prospects, and implications for. *J. Phys. G*, 50(4):045003, 2023. doi:10.1088/1361-6471/acab1d.
- [65] Bigeng Wang. Calculation of the $K_L - K_S$ mass difference for physical quark masses. *PoS, LATTICE2019:093*, 2019. doi:10.22323/1.363.0093.
- [66] Bigeng Wang. Calculating Δm_K with lattice QCD. *PoS, LATTICE2021:141*, 2022. doi:10.22323/1.396.0141.
- [67] O. Deschamps, S. Descotes-Genon, S. Monteil, V. Niess, S. T’Jampens, and V. Tisserand. The Two Higgs Doublet of Type II facing flavour physics data. *Phys. Rev. D*, 82:073012, 2010. doi:10.1103/PhysRevD.82.073012.
- [68] Debtosh Chowdhury and Otto Eberhardt. Update of Global Two-Higgs-Doublet Model Fits. *JHEP*, 05:161, 2018. doi:10.1007/JHEP05(2018)161.
- [69] Pere Arnan, Damir Bečirević, Federico Mescia, and Olcyr Sumensari. Two Higgs doublet models and $b \rightarrow s$ exclusive decays. *Eur. Phys. J. C*, 77(11):796, 2017. doi:10.1140/epjc/s10052-017-5370-z.
- [70] Mayumi Aoki, Shinya Kanemura, Koji Tsumura, and Kei Yagyu. Charged higgs bosons in the minimal supersymmetric standard model (mssm): Updated constraints and experimental prospects. *Physical Review D*, 80(1):015017, 2009.
- [71] F. Mahmoudi and O. Stal. Flavor constraints on the two-higgs-doublet model of type iii. *Physical Review D*, 81(3):035016, 2010.
- [72] Martin Jung, Antonio Pich, and Paula Tuzon. Implications of lhcb measurements and future prospects. *European Physical Journal C*, 74(9):268, 2014.

- [73] Andrzej J. Buras and Fulvia De Fazio. 331 Models Facing the Tensions in $\Delta F = 2$ Processes with the Impact on ε'/ε , $B_s \rightarrow \mu^+\mu^-$ and $B \rightarrow K^*\mu^+\mu^-$. *JHEP*, 08:115, 2016. doi:10.1007/JHEP08(2016)115.
- [74] Andrzej J. Buras, Pietro Colangelo, Fulvia De Fazio, and Francesco Loparco. The charm of 331. *JHEP*, 10:021, 2021. doi:10.1007/JHEP10(2021)021.
- [75] Martin S. Lang and Ulrich Nierste. $B_s \rightarrow \mu^+\mu^-$ in a two-Higgs-doublet model with flavour-changing up-type Yukawa couplings. *JHEP*, 04:047, 2024. doi:10.1007/JHEP04(2024)047.
- [76] Yasmine Sara Amhis et al. Averages of b-hadron, c-hadron, and τ -lepton properties as of 2021. *Phys. Rev. D*, 107(5):052008, 2023. doi:10.1103/PhysRevD.107.052008.
- [77] Dipankar Das. New limits on $\tan \beta$ for 2HDMs with Z_2 symmetry. *Int. J. Mod. Phys. A*, 30(26):1550158, 2015. doi:10.1142/S0217751X15501584.
- [78] Francesca Borzumati and C. Greub. Lessons from anti-B \rightarrow X(s) γ in two Higgs doublet models. In *29th International Conference on High-Energy Physics*, pages 1735–1739, 10 1998.
- [79] Marco Ciuchini, G. Degrossi, P. Gambino, and G. F. Giudice. Next-to-leading QCD corrections to $B \rightarrow X_s \gamma$: Standard model and two Higgs doublet model. *Nucl. Phys. B*, 527:21–43, 1998. doi:10.1016/S0550-3213(98)00244-2.
- [80] A. Arbey, F. Mahmoudi, O. Stal, and T. Stefaniak. Status of the Charged Higgs Boson in Two Higgs Doublet Models. *Eur. Phys. J. C*, 78(3):182, 2018. doi:10.1140/epjc/s10052-018-5651-1.
- [81] Oliver Atkinson, Matthew Black, Alexander Lenz, Aleksey Rusov, and James Wynne. Cornering the Two Higgs Doublet Model Type II. *JHEP*, 04:172, 2022. doi:10.1007/JHEP04(2022)172.
- [82] Tetsuya Enomoto and Ryoutaro Watanabe. Flavor constraints on the Two Higgs Doublet Models of Z_2 symmetric and aligned types. *JHEP*, 05:002, 2016. doi:10.1007/JHEP05(2016)002.
- [83] M. Misiak, Abdur Rehman, and Matthias Steinhauser. Towards $\bar{B} \rightarrow X_s \gamma$ at the NNLO in QCD without interpolation in m_c . *JHEP*, 06:175, 2020. doi:10.1007/JHEP06(2020)175.
- [84] Howard E. Haber and Deva O’Neil. Theoretical constraints on the higgs potential in the two higgs doublet model. *Physical Review D*, 83(3):055017, 2011.
- [85] Palash B. Pal. The Strong CP question in $SU(3)(C) \times SU(3)(L) \times U(1)(N)$ models. *Phys. Rev. D*, 52:1659–1662, 1995. doi:10.1103/PhysRevD.52.1659.
- [86] A. Barroso, P. M. Ferreira, I. P. Ivanov, and Rui Santos. Metastability bounds on the two Higgs doublet model. *JHEP*, 06:045, 2013. doi:10.1007/JHEP06(2013)045.
- [87] I. F. Ginzburg and I. P. Ivanov. Tree-level unitarity constraints in the most general 2HDM. *Phys. Rev.*

D, 72:115010, 2005. doi:10.1103/PhysRevD.72.115010.

- [88] Ning Chen, Tao Han, Shufang Su, Wei Su, and Yongcheng Wu. Type-II 2HDM under the Precision Measurements at the Z -pole and a Higgs Factory. *JHEP*, 03:023, 2019. doi:10.1007/JHEP03(2019)023.
- [89] Tao Han, Shuailong Li, Shufang Su, Wei Su, and Yongcheng Wu. Comparative Studies of 2HDMs under the Higgs Boson Precision Measurements. *JHEP*, 01:045, 2021. doi:10.1007/JHEP01(2021)045.